Preparation and Electrical Properties of $Eu(II)_xNb(IV)O_{2+x}$

Kenji Ishikawa, Gin-ya Adachi,* and Jiro Shiokawa
Department of Applied Chemistry, Faculty of Engineering, Osaka University, Yamadaoka, Suita, Osaka 565
(Received March 17, 1982)

Nonstoichiometric compounds, Eu_xNbO_{2+x}, were prepared. A cubic tungsten bronze type structure was found in the single phase region of Eu_xNbO_{2+x} ($0.5 \leqq x \leqq 1.0$). Magnetic susceptibility measurements showed that the oxidation state of europium in the bronzes was bivalent. The Eu_xNbO_{2+x} was a metallic conductor in the temperature range 4.2—300 K. Thermoelectromotive force measurements (100—350 K) indicated that the charge carriers were electrons and that the effective mass of the electrons increased with decreasing x in Eu_xNbO_{2+x}.

Europium niobium bronzes, Eu_xNbO_{2+x}, where x lies between 0.50 and 1.00 are tungsten bronze type compounds. At values of x greater than 0.65, the niobium bronzes crystallize in the cubic tungsten bronze type structure and exhibit the metallic properties of bluish luster and electronic conduction.[1,2] At values of x less than 0.65, the structure is the tetragonal tungsten bronze type and the bronzes are nonmetallic.[1-5] In the bronzes, Nb^{4+} ions co-exist with Nb^{5+} ions and the number of Nb^{4+} ions, which is equal to the number of conduction electrons for the cubic bronzes, is controlled simply by controlling the europium concentration, since the bronzes are expressed by a formula $Eu^{2+}Nb^{4+}_{2x-1}Nb^{5+}_{2-2x}O^{2-}_3$. However, the number of Nb^{4+} ions is also controlled by removing lattice oxygens from the bronzes, and the lattice oxygen should be removed until all the Nb^{5+} ions is reduced to Nb^{4+}, *i.e.*, $Eu^{2+}_x Nb^{4+}O^{2-}_{2+x}$. In this paper chemical and physical properties of Eu_xNbO_{2+x} are discussed and compared with those of Eu_xNbO_3.

Experimental

Preparative. A fully mixed powder of Eu_2O_3 (purity 99.9%: Shin-etsu Chemical Co.,), Nb_2O_5 (purity 99.9%: Wako Chemical Industries, Ltd.,), and Nb (purity 99.9%: Wako Chemical Industries, Ltd.,) was pressed into pellets. The pellets were packed into a Mo box and sealed in a silica tube under vacuum. The pellets were degassed under vacuum at 450 K for 3 h before the sealing procedure. The silica tube was set up in a vertical furnace and heated at 1423—1473 K for 6 h. The sample was ground in an agate mortar, re-pressed into pellets, degassed, sealed in a silica tube under vacuum, and heated again at 1423—1473 K for 30 h. The reaction was completed during the procedure described above and assumed to proceed as follows.

$$0.5xEu_2O_3 + (0.4-0.1x)Nb_2O_5 + (0.2+0.2x)Nb \longrightarrow Eu_xNbO_{2+x} \quad (1)$$

However, in practice a small excess of niobium metal was used to compensate for a slight oxidation of the samples during the synthetic procedure.

Analyses. The phase purity and the structure type of the samples were analyzed by X-ray powder diffraction with a Rigaku Denki "Rotor-flex diffractometer."

The Eu/Nb ratios, namely x in Eu_xNbO_{2+x}, were determined by fluorescence X-ray analysis with a Rigaku Denki "Ultra Trace unit," and the O/Nb ratios were obtained by weighing the samples before and after complete oxidation and assuming the following oxidation reaction,

$$Eu_xNbO_{2+x} + 0.25(x+1)O_2 \longrightarrow 0.5xEu_2O_3 + 0.5Nb_2O_5. \quad (2)$$

Magnetic and Electrical Measurements. The magnetic moments of the samples were obtained from magnetic susceptibility measurements with a Shimadzu magnetic balance "MB-11" under a He atmosphere in the temperature range 4.2 to 300 K.

Electrical resistivity measurements were done for the polycrystalline sintered bars with a simple four-probe d.c. method in a helium atmosphere from 4.2 to 300 K. The heating rate of each measurement was below 1 K/min. The dc currents was produced with a Takeda Riken dc generator "TR-6141," and the potential difference between the two potential leads was recorded with a Yokogawa Denki "Type 3036 X-Y recorder;" the resistivity measurements were carried out in the ohmic region of the current. Since the measured voltage included a thermally generated emf, the dc current was stopped at regular time intervals and the emf was separated. The shape and size of the samples and the attachment of electrical leads used were the same as those described in the previous paper.[1]

Thermoelectric Power Measurements. Thermoelectric powers of the rectangular samples of about 2 mm^2 in cross section and about 4 mm long were measured under a He atmosphere in the range 100—373 K. The temperature difference between both side of the sample was adjusted to fall within 10 K. The absolute Seebeck coefficient was obtained after compensating the emf of copper action as the electrode of our apparatus and given according to the following equation:

$$S = S_{Cu} - \Delta V/\Delta T, \quad (3)$$

where S_{Cu} was the absolute Seebeck coefficient of Copper,[6] ΔV was the thermoelectric voltage of the sample, and ΔT was the temperature difference between both sides of the samples.

Results and Discussion

The phases and analytical data for Eu_xNbO_{2+x} and Eu_xNbO_3 obtained are listed in Table 1, which shows that the single phase region of Eu_xNbO_{2+x} is from $x=0.5$ to $x=1.0$. The niobium bronze Eu_xNbO_3 of $x=0.50$—0.65 has a tetragonal form[1-5] and for $x=0.65$—1.00 has a cubic form,[1,2] while Eu_xNbO_{2+x} has a cubic form in the single phase region.

Lattice constants of the cubic phased Eu_xNbO_{2+x} and Eu_xNbO_3 are plotted in Fig. 1 as a function of the europium concentration x. The lattice constants of Eu_xNbO_3 increases almost linearly with an increase in x.[2] The least-squares fitting generates the following equation:

$$a(\text{cubic}) = 3.874 + 0.1515x(\text{Å}). \quad (4)$$

Lattice constants of Eu_xNbO_{2+x} also increase with an increase in x in the range from $x=0.5$ to $x=1.0$, but

Table 1. Analytical and crystal data for Eu_xNbO_3 and Eu_xNbO_{2+x}

Exptl No.	Eu_xNbO_y (nominal) x	y	Eu_xNbO_y (analytical) x	y	Phase	a(cubic) Å	a(tetragonal) Å	c(tetragonal) Å
Eu_xNbO_3								
A	1.00	3.00	1.01	3.01	Cubic	4.026		
B	0.90	3.00	0.90	3.00	Cubic	4.010		
C	0.85	3.00	0.88	3.03	Cubic	4.009		
D	0.80	3.00	0.82	3.03	Cubic	4.002		
E	0.75	3.00	0.76	3.03	Cubic	3.985		
F	0.70	3.00	0.70	3.09	Cubic	3.980		
G	0.65	3.00	0.68	3.05	Cubic	3.978		
H	0.60	3.00	0.60	3.03	Tetragonal	—	12.361	3.885
I	0.55	3.00	0.58	3.02	Tetragonal	—	12.363	3.892
J	0.50	3.00	0.51	3.02	Tetragonal	—	12.355	3.901
Eu_xNbO_{2+x}								
A	1.00	3.00	1.01	3.01	Cubic	4.026		
K	0.90	2.90	0.90	2.94	Cubic	4.013		
L	0.80	2.80	0.79	2.93	Cubic	3.993		
M	0.70	2.70	0.71	2.82	Cubic	3.992		
N	0.60	2.60	0.62	2.70	Cubic	3.983		
O	0.50	2.50	0.52	2.66	Cubic	3.977		
P	0.50	2.50	0.51	2.47	Cubic+u[a)]	3.988		
Q	0.45	2.45	0.47	2.38	Cubic+u	3.990		
R	0.40	2.40	0.42	2.39	Cubic+u	3.982		
S	0.30	2.30	0.30	2.16	Cubic+u	3.982		

a) u: Unknown phase.

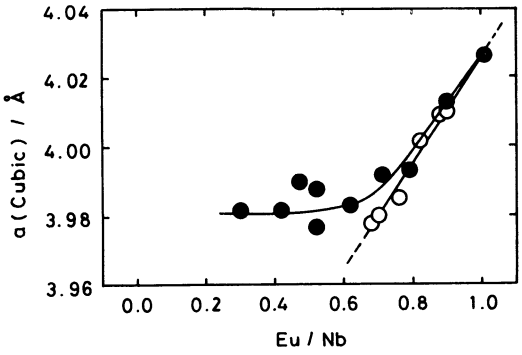

Fig. 1. Lattice constants *vs.* Eu concentration for Eu_xNbO_3 (○) and Eu_xNbO_{2+x} (●).

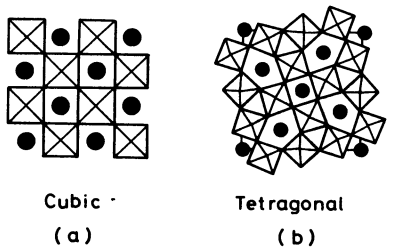

Fig. 2. Schematic diagram for the cubic and the tetragonal Eu_xNbO_3.
The bivalent europium cation can occupy the positions expressed by the black circles.

the change is not linear and the constants of Eu_xNbO_{2+x} are greater than those of Eu_xNbO_3 on a fixed composition especially below $x=0.7$. Below $x=0.5$, an unknown phase appeared in addition to a cubic phase of $a=3.982$ Å, and the tetragonal phase which was found in the Eu_xNbO_3 of $x=0.5$—0.65 was not observed.

The phase change of Eu_xNbO_3 from a cubic to a tetragonal form is explained as follows. The crystal structure of the cubic and the tetragonal niobates are revealed in Figs. 2 (a) and (b). A bivalent europium cation occupies a body-centered site of the cubic lattice (Fig. 2 (a)) and the site expressed by the black circle in the tetragonal cell (Fig. 2 (b)). Since the lattice constant decreases with a decrease in the europium concentration for the cubic Eu_xNbO_3, the maximum ionic radius to be able to occupy the body-centered site of the perovskite structure also decreases with decreasing the europium concentration, and at $x=0.65$ the maximum ionic radius becomes equal to the ionic radius of Eu^{2+}. At $x=0.65$, the lattice constant "a" is 3.987 ± 3 Å and the tolerance factor[7] "t" is 1.01. The tolerance factor is defined by the following equation:

$$t = (r(Eu^{2+}) + r(O_2^-))/\sqrt{2}\,a, \qquad (5)$$

where $r(Eu^{2+})$ (1.45 Å: 6th coordination) and $r(O^{2-})$ (1.40 Å: 6th coordination) are ionic radii[8] of Eu^{2+} and O^{2-} and a (3.987 Å for $Eu_{0.65}NbO_3$) is a cubic lattice constant. Below $x=0.65$ $t>1$, the body-centered site of the cubic Eu_xNbO_3 can no longer accomodate a bivalent europium cation, and the cubic phase transforms to the tetragonal phase. This can provide room for a bivalent europium cation in the limited range from $x=0.5$ to $x=0.65$.[1-5]

The above discussion is also applicable to Eu_xNbO_{2+x}. The lower limit of the lattice constant for the cubic Eu_xNbO_{2+x} seems to be almost the same as the lattice size of $Eu_{0.65}NbO_3$. However, the tetragonal phase,

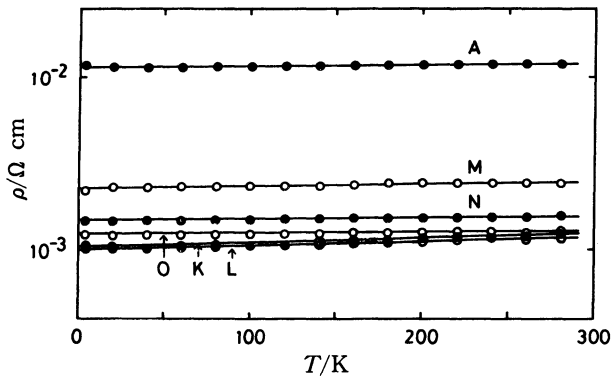

Fig. 3. Temperature dependence of resistivity for Eu_xNbO_{2+x}.
A—O are experimental number in Tables 1 and 2.

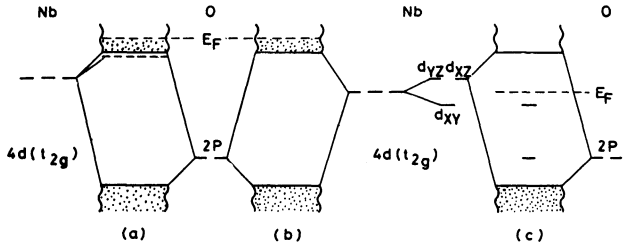

Fig. 4. Energy-level diagram for Eu_xNbO_{2+x} and Eu_xNbO_3.

which was found for Eu_xNbO_3 at $x=0.5$—0.65, was not found and an unknown phase was detected in the Eu_xNbO_{2+x} below $x=0.5$.

The electrical resistivity measurements for Eu_xNbO_{2+x} (Fig. 3) show that the cubic Eu_xNbO_{2+x} is a metallic conductor at $x=0.5$—1.0. These results are different from those of Eu_xNbO_3 in a low x region. In the case of Eu_xNbO_3, semiconduction was observed for the cubic samples at $x=0.5$—0.65[1-5] and metallic conduction was observed for the cubic samples at $x=0.65$—1.0.[1,2]

The difference in the electrical conduction between Eu_xNbO_{2+x} and Eu_xNbO_3 at $x=0.5$—0.65 is related to the distinction in their crystal structure. The difference on conduction manner owing to the structural difference was already discussed for Eu_xNbO_3 with a band model in the previous paper.[1]

An energy level diagram for Eu_xNbO_{2+x} is proposed in Fig. 4, which is assembled on the basis of Goodenough's model for Na_xWO_3.[9] The conduction band is composed of $4d(t_{2g})$ orbitals of niobium and 2p orbitals of oxygen. The $4d(t_{2g})$ levels of niobium, which are composed of $4d(t_{2g})$ orbitals around oxygen vacancies, are located below the conduction band.

The number of conduction electrons is equal to the number of Nb^{4+} as for Eu_xNbO_3,[1] and there is a Nb^{4+} per one formula of Eu_xNbO_{2+x}. Therefore, Eu_xNbO_{2+x} exhibits a metallic conduction (Fig. 3) as the cubic Eu_xNbO_3. However the mobility of an electron and an effective mass of electron for Eu_xNbO_{2+x} should be

Table 2. Magnetic and electrical data for Eu_xNbO_3 and Eu_xNbO_{2+x}

Exptl No.	Eu_xNbO_y (analytical) x	y	Magnetic moments μ_{eff} (μ_B) (Obsd)	μ_{eff}[a] (μ_B) (Calcd)	μ_{eff}[b] (μ_B) (Calcd)	Conduction	S[c] $\mu V K^{-1}$	S_0[d] $\mu V K^{-1}$	m^*/m_0[e]
Eu_xNbO_3									
A	1.01	3.01	7.92	8.16	7.98	m[f]	−7.0	−3.26	2.1
B	0.90	3.00	7.61	7.68	7.52	m	−6.2	−3.77	1.6
C	0.88	3.03	7.36	7.58	7.45	m	−8.2	−4.10	2.0
D	0.82	3.03	7.16	7.31	7.19	m	−11.1	−4.63	2.4
E	0.76	3.03	6.80	7.03	6.92	m	−14.7	−5.36	2.7
F	0.70	3.09	6.34	6.69	6.64	m	−17.2	−8.74	2.0
G	0.68	3.05	6.46	6.61	6.54	m	−22.2	−7.81	2.8
H	0.60	3.03	6.04	6.18	6.15	s[g]	−182	—	—
I	0.58	3.02	5.89	6.07	6.05	s	−152	—	—
J	0.51	3.02	5.47	5.67	5.67	s	—	—	—
Eu_xNbO_{2+x}									
A	1.01	3.01	7.92	8.16	7.98	m	−7.0	−3.26	2.1
K	0.90	2.94	7.70	7.71	7.53	m	−6.2	−3.42	1.8
L	0.79	2.93	7.15	7.21	7.06	m	−8.3	−3.99	2.1
M	0.71	2.82	6.69	6.87	6.70	m	−12.9	−3.77	3.4
N	0.62	2.70	6.29	6.47	6.27	m	−12.8	−3.56	3.6
O	0.52	2.66	5.70	5.89	5.70	m	−18.8	−3.99	4.7
P	0.51	2.47	5.74	5.94	5.66	—	—	—	—
Q	0.47	2.38	5.50	5.73	5.41	—	—	—	—
R	0.42	2.39	5.22	5.47	5.18	—	—	—	—
S	0.30	2.16	4.36	4.77	4.35	—	—	—	—

a) μ_{eff} (calcd)$=\sqrt{x\mu^2(Eu^{2+})+(Nb^{4+}/Nb)\mu^2(Nb^{4+})}$; μ (Eu^{2+})$=7.94\mu_B$; μ (Nb^{4+})$=1.73\,\mu_B$. b) μ_{eff} (calcd)$=\sqrt{x}\mu(Eu^{2+})$.
c) S: Observed absolute Seebeck coefficient at 300 K. d) S_0: Calculated absolute Seebeck coefficient at 300 K. e) m^*: Effective mass of electron; m_0: rest mass of electron. f) m: Metallic. g) s: Semiconductive.

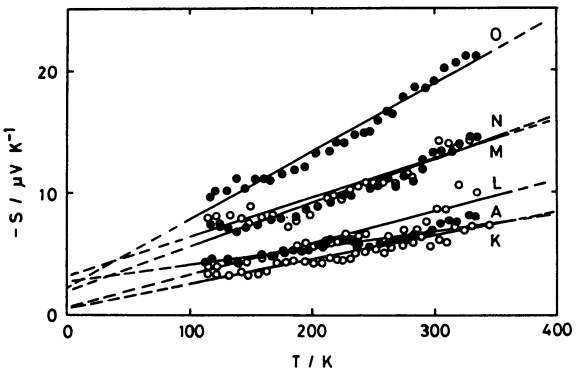

Fig. 5. Temperature dependence of the Seebeck coefficient for Eu_xNbO_{2+x}.
A—O are experimental number in Tables 1 and 2.

different from those for Eu_xNbO_3, since positive charged oxygen vacancies are considered to attract the conduction electrons around the vacancies electrostatically.

The effective masses of electrons for metallic Eu_xNbO_{2+x} are roughly evaluated by a thermoelectric power measurement, assuming that all the 4d electrons of niobium are concerned to the electrical conduction. For the free-electron approximation, the Seebeck coefficient is given by the relation:[10]

$$S = \frac{2}{3}\left(\frac{\pi}{3}\right)^{2/3} \frac{m^* k^2 T}{e(h/2\pi)^2} N^{-2/3}. \quad (6)$$

The effective mass is obtained by comparison of the observed Seebeck coefficient with the calculated value ($m^* = m_0$). Figure 5 shows that the Seebeck coefficient of Eu_xNbO_{2+x} at various temperatures. Temperature dependence of the Seebeck coefficient for each Eu_xNbO_{2+x} is almost linear and this fact suggests that the behavior of the conduction electrons resemble that of the free electrons. The Seebeck coefficient of Eu_xNbO_{2+x} increases with decreasing x at each temperature (Fig. 5). The increase in the Seebeck coefficient means that the effective mass of the electrons of Eu_xNbO_{2+x} increases with decreasing x. In Table 2, effective electric masses of Eu_xNbO_{2+x} and Eu_xNbO_3 are listed. The effective electric mass for Eu_xNbO_{2+x} increases with decreasing x from $2m_0$ to $5m_0$. However, the effective mass for Eu_xNbO_3 is independent of x and about $2m_0$ for any sample obtained. An interpretation for the disagreement in masses of Eu_xNbO_{2+x} and Eu_xNbO_3 is as follows. The host lattice of Eu_xNbO_3, namely NbO_3, where the conduction electrons go through, is not changed with x, and the effective mass is not affected by x. On the other hand, Eu_xNbO_{2+x} has oxygen vacancies, and the lattice of Eu_xNbO_{2+x} is fairly different from that of Eu_xNbO_3 at low x. The conduction electrons are trapped near the oxygen vacancies through the electrostatic force; the electrostatic interaction of the electrons with the vacancies is strong at low x, because there exist many vacancies at low x. This is the reason why the effective mass of the electrons for Eu_xNbO_{2+x} increases with decreasing x.

References

1) K. Ishikawa, G. Adachi, M. Hasegawa, K. Sato, and J. Shiokawa, *J. Electrochem. Soc.*, **128**, 1374 (1981).
2) G. V. Bazuev, O. V. Makarova, and G. P. Shveikin, *Dokl. Akad. Nauk SSSR*, **223**, 358 (1975).
3) F. Studer, J. P. Fayolle, and B. Raveau, *Mater. Res. Bull.*, **11**, 1125 (1976).
4) F. Studer, G. Allais, and B. Raveau, *J. Phys. Chem. Solids*, **41**, 1187 (1980).
5) F. Studer, G. Allais, and B. Raveau, *J. Phys. Chem. Solids*, **41**, 1199 (1980).
6) N. Cusack and P. Kendall, *Proc. Phys. Soc.*, **72**, 898 (1958).
7) J. B. Goodenough and J. A. Kafalas, *J. Solid State Chem.*, **6**, 493 (1973).
8) R. D. Shannon, *Acta Crystallogr., Sect. A*, **32**, 751 (1976).
9) J. B. Goodenough, "Metallic Oxide," in "Progress in Solid State Chemistry," ed by H. Reiss, Pergamon, Oxford New York (1972), Vol. 5.
10) B. L. Crowder and M. J. Sienko, *J. Chem. Phys.*, **38**, 1576 (1963).